Appl. Phys. B 29, 235–250 (1982)

Applied Physics B Photophysics and Laser Chemistry

Low-Temperature Spectroscopy of Organic Molecules in Solids by Photochemical Hole Burning

L. A. Rebane

Institute of Chemical Physics and Biophysics, Estonian Academy of Sciences,
SU-200104 Tallinn, USSR

A. A. Gorokhovskii and J. V. Kikas

Institute of Physics, Estonian Academy of Sciences, SU-202400 Tartu, USSR

Received 5 June 1982/Accepted 15 July 1982

Abstract. Characteristic features of photochemical hole-burning (PHB) in the impurity spectra of low-temperature solids and PHB applications in molecular spectroscopy are considered. The evolution of a no-phonon hole and a phonon sidehole in excitation and fluorescence spectra is analysed on the basis of model calculations. Some more complex models for PHB are considered, which take into account reverse reactions, the optical thickness of the sample, the inhomogeneous dispersion of both homogeneous linewidths and transition energies of the photoproduct and quasi-static impurity-impurity interactions. The effects of PHB on fluorescence line narrowing are discussed. By PHB homogeneous linewidths of purely electronic and vibronic no-phonon lines in the spectra of some porphine and phthalocyanine derivatives in various matrices are measured and their temperature dependence is studied. The latter is found to be essentially different in polycrystalline and glassy matrices. Line-broadening mechanisms are discussed. By PHB the existence of an inhomogeneous distribution of vibrational frequencies in molecular impurities is established. The applications of PHB in the studies of photochemical reactions in solid solutions of phthalocyanine derivatives and tetracene are regarded and the mechanisms of these reactions are discussed. The results obtained by PHB for chlorophyll and its derivatives are presented.

PACS: 78.50

The main progress in todays molecular spectroscopy consists in the elimination of the inhomogeneous broadening (IHB) of optical spectra. For complex organic molecules embedded in solid organic matrices the IHB is so large that most important details of the spectrum of individual molecules are completely hidden [1–3]. In this paper we shall discuss a possibility of overcoming the inhomogeneous broadening by means of burning persistent narrow spectral holes in inhomogeneously broadened spectral bands. A simple idea of using selective bleaching of photochemically unstable molecules under monochromatic laser excitation in order to reveal the homogeneous structure of the spectra was first demonstrated by our group in 1974 on an example of a frozen solution of a free-base phthalocyanine (H_2Pc) in *n*-octane at 5 K [4]. The spectral hole was obtained in the 694.0 nm component of a 0–0 multiplet after irradiating the sample with a ruby laser. The half-width of the hole was 0.07 cm^{-1}. It is as much as 100 times narrower than that of the inhomogeneously broadened component of the multiplet indicating the existence of very narrow pure-electronic no-phonon lines (NPL) in the spectra of complex organic molecules. The hole persisted in darkness for many hours (the lifetime of the photoproduct). The burning of persistent holes gives an opportunity to perform spectral measurements in resonance with the excitation without applying any time-resolving devices.

By now the persistent spectral holes induced by photochemical transformations of the molecule (commonly referred to as photochemical hole burning, PHB) have been observed in a large number of various molecules in various matrices [5–19], including important biochemical molecules such as chlorophyll [20–24]. It is evident that mechanisms of photochemical hole burning may be rather different, including phototautomerization [4–7, 10–12], photodissociation [8, 9], rearrangement of hydrogen bonds [15–17], etc. In some cases the phototransformation and formation of a hole were obtained as a result of a two-step excitation [24, 25].

After the pioneering work by Kharlamov et al. [26] spectral holes were also burned in the bands of photochemically stable molecules, such as aromatic hydrocarbons embedded in organic glasses [27–30]. As there is one-step excitation of molecules which is not followed by any photochemical change of guest molecules, the hole burning mechanism for these cases is referred to as photophysical or nonphotochemical hole burning (NPHB). It has been interpreted as being due to tunnelling processes in glassy materials. However, the problem of the classification of hole-burning mechanisms is rather subtle – there are cases where both host matrix and guest molecule participate actively (rearrangement of hydrogen bonds between them [16]). It is possible to accept a more general viewpoint and consider the guest molecule and its surrounding as a new physical entity – impurity centre. Then PHB and NPHB turn out to be the limiting cases of a large variety of phototransformations of impurity centres and the difference between them in many cases is unessential. In what follows we concentrate mainly on systems where the photochemical nature of hole burning is well established, but many of our results are of a wider application.

The specific features of PHB are clearly displayed when compared with the selective saturated hole burning [31–33]. A saturated hole in the IHB band arises if irradiation is of sufficient intensity to saturate a transition in a two-level system. The hole burned photochemically differs from the saturated hole in two points of principal importance. First, photochemical transformation takes place at every act of photon absorption (with a certain probability) and the summary effect (a hole) is proportional to the irradiation dose, whereas the saturation of the transition depends on irradiation intensity. Secondly, the lifetime of the photochemical hole is determined only by that of the photoproduct, whereas the lifetime of the saturated hole corresponds to the lifetime of the excited state[1]. But since the hole is formed as a result of the decrease in the finite number of absorbing centers at the irradiation frequency, the hole profile in both cases displays the effects of saturation broadening. It should be noted that an increase of the triplet state population due to the single-to-triplet convertion brings about a hole in the singlet band [34, 35].

Evidently, the PHB kinetics is strictly dependent on the relation between the homogeneous and inhomogeneous intensity distribution in a spectrum of impurity molecules. Let us recall here some parameters for an abstract system, keeping in mind a frozen solution of organic molecules. In accordance with the theory [36] the main feature of a homogeneous spectrum of electronic absorption is the existence of extremely narrow NPL and a comparatively broad ($\Gamma_p \sim 100\,\mathrm{cm}^{-1}$) phonon sideband (PSB). The total homogeneous linewidth (HLW) Γ of NPL depends on the time T_1 of the excited level population decay and on the dephasing time T_2' as follows [37]:

$$\Gamma = \frac{1}{T_1} + \frac{2}{T_2'}. \tag{1}$$

For a pure-electronic NPL the limit value of Γ at 0 K should be of the order of $10^{-3}\,\mathrm{cm}^{-1}$ [36].

At helium temperatures the absorption in the maximum of homogeneous NPL exceeds manytimes that in PSB. For an estimation one may take the Debye-Waller factor $\alpha = 1/2$ that leads to the ratio $I_{\mathrm{NPL}}/I_{\mathrm{PSB}} \approx \Gamma_p/\Gamma \approx 10^5$. For the NPL of a vibronic transition one may take $\Gamma = 0.1 \div 1\,\mathrm{cm}^{-1}$ and then $I_{\mathrm{NPL}}/I_{\mathrm{PSB}} \approx 10^2 \div 10^3$. Such high relative intensities of NPL have never been observed in real spectra because of IHB. With the width of the IHB band $\Delta = 1 \div 100\,\mathrm{cm}^{-1}$ one obtains a decrease in the ratio $I_{\mathrm{NPL}}/I_{\mathrm{PSB}}$ in the spectra by a factor of $\Delta/\Gamma = 10^2 \div 10^5$.

Narrow NPL of a high peak intensity make PHB very selective: it results in the formation of narrow no-phonon holes, which are very sensitive to all kinds of interactions that affect the width and position of NPL.

Because of the broad PSB no monochromatic excitation can be totally selective, and it will be absorbed in two ways: selectively, by molecules whose NPL are in resonance, and unselectively, by molecules whose PSB overlap at the excitation frequency. Due to a great difference in the absorption via NPL and PSB, and

---

[1] The differences between saturated and photochemical holes become unessential when the lifetime of a photoproduct is comparable with the optical lifetime

photochemical bleaching the relation between these two groups changes in the course of irradiation in favour of unselectively excited molecules, which brings about the appearance of broad holes (hole sidebands) in the hole spectrum as well.

For a correct distinction of a HLW (as well as other homogeneous parameters) from the corresponding PHB experiment one needs model calculations that take into account saturation effects, i.e. the change of the hole with the irradiation dose. It is important to include in a model also possible feedback processes (e.g. thermal decomposition of the photoproduct) that bring about the limit of saturated-holes profiles. A realistic model should take into account also the presence of PSB.

Theoretical models of the PHB process were discussed by Gorokhovskii and Kikas [38], Voelker et al. [39], and de Vries and Wiersma [40]. They have calculated the narrow no-phonon hole broadening caused by saturation effects. The appearance of phonon wings in the hole spectrum has been considered by Friedrich et al. [41]. In Sect. 1 we shall discuss models that describe the transient change in the inhomogeneous distribution of the impurity centers in selective photochemistry (the hole formation process), taking into account all three factors: saturation effects, phonon wings and reverse processes. We shall discuss the influence of other factors, such as higher-dimensional spectral inhomogeneity, impurity-impurity interaction, etc. on the hole burning process. Next the appearance of holes in luminescence and excitation spectra as well as the effects of hole-burning on the fluorescence line narrowing will be considered. In view of PHB applications the hole formation in an optically dense sample will also be considered.

PHB is now successfully used for various purposes of molecular and solid state spectroscopy. Let us give here a brief account of the problems that may be or have already been solved by this method.

The most accurate measurements of HLW of the pure-electronic NPL have been done with PHB for impurity molecules of H_2Pc and its derivatives in crystalline matrices [10, 42, 43], for free-base porphin in *n*-octane [39, 44] and decane [7], for dimethyl-*s*-tetrazine in durene [8] and *s*-tetrazine in benzene [9], and for zinc porphin in octane [35]. It has been shown that for these complex molecules the limit value of HLW is extremely narrow ($\Gamma \approx 10^7$ Hz) and coincides with the radiative linewidth, that is of principal importance.

The broadening of HLW with temperature was first obtained in the region of $T < 30$ K and the dephasing of the excited electronic state of molecules due to electron-phonon coupling has been investigated [7, 10, 39, 42–44]. The data indicate that a pseudo-local vibration plays an overwhelming role in the dephasing processes.

Dephasing processes are quite successfully investigated by nonlinear optical methods (photon echo, etc.) [45]. Recently, for pentacene in naphthalene the difference between T_2 and $2T_1$ was obtained below 2 K [46]. We believe that our knowledge of dephasing processes will be improved by comparing the experimental data obtained from PHB and the methods of coherent optics.

The low-temperature intramolecular vibrational relaxation of an excited vibronic state can be investigated when burning a hole in the IHB vibronic band. Some important information about the elementary channels of vibrational relaxation has been obtained this way [9, 47, 48].

When a hole is burned in an inhomogeneous distribution of impurities, a spectrum of holes appears, the position of which is shifted from the resonance at the frequencies of all active molecular vibrations [13, 17, 28, 49]. On the contrary, when burning a hole in a vibronic band, a manifolding of holes in the pure electronic band is observed [47]. From these experiments, besides the data on the vibrational frequencies of impurity molecules, a fine noncorrelation effect can be distinguished – a small difference in the vibrational frequency of guest molecules, which have coincident frequencies of a pure-electronic transition [11].

Very narrow holes were used as a probe for the structure of the matrix [25, 35, 39], including amorphous solids [25, 43, 50].

From the hole burning kinetics the information about the photochemical reactions and the reverse processes can be obtained [24, 25, 27, 38], especially when the spectrum of the photoproduct is observed [5, 6, 21, 22, 51].

PHB may likely be applied to the observation of very small level splittings, otherwise hidden by inhomogeneity [13, 52], as well as for distinguishing isotopic, isomeric, and other fine structures. In all these cases the manifolding of holes should be observed.

In Sect. 2 we shall review the PHB application results obtained in our laboratory.

1. Process of Hole-Burning

1.1. Basic Model

To consider the hole-burning process, particularly, the evolution of the hole contour in the burning process, we start from a simple model based on the following assumptions:

(i) weak excitation providing the absence of optical saturation;

(ii) low impurity concentration insuring the absence of impurity-impurity interactions, e.g. energy transfer;
(iii) small optical thickness of a sample that makes possible its uniform irradiation by monochromatic light of frequency ν_0 and intensity I_0;
(iv) one-dimensional inhomogeneity: only the frequency of purely electronic transitions, ω, is supposed to vary for different impurities. The homogeneous spectra of absorption $\kappa(\nu-\omega)$ and luminescence $\varphi(\nu-\omega)$ are supposed to be shifted without any distortion of their shapes and without changes in their integral intensity. The latter implies a similar orientation of all impurities and equal values of the integral absorption cross section σ, as well as quantum yields η and η_f of photochemistry and fluorescence, respectively. Statistical spectral properties of such a system are then fully described by the generally time-dependent inhomogeneous distribution function (IDF) $\varrho(\omega, t)$;
(v) one-photon mechanism of photochemistry;
(vi) stability of photoproducts that guarantees the irreversibility of the hole burning process;
(vii) large photochromic shift as compared to the width of homogeneous spectrum. This prevents the disturbance of the hole by the redistribution of burned-out impurities.
The kinetics of hole-burning is governed then by the simple equation

$$\dot{\varrho}(\omega, t) = -I_0\sigma\kappa(\nu_0-\omega)\eta\varrho(\omega, t), \qquad (2)$$

which yields

$$\varrho(\omega, t) = \varrho(\omega, 0)\exp[-I_0\sigma\kappa(\nu_0-\omega)\eta t]. \qquad (3)$$

The spectra of excitation, $I_e(\nu, t)$, and fluorescence (at broad-band excitation), $I_f(\nu, t)$, depend on the burning time t and are given by

$$I_e(\nu, t) = I\sigma\eta_f \int_{-\infty}^{\infty} \kappa(\nu-\omega)\,\varrho(\omega, t)\,d\omega \qquad (4)$$

and

$$I_f(\nu, t) = \bar{I}\sigma\eta_f \int_{-\infty}^{\infty} \varphi(\nu-\omega)\,\varrho(\omega, t)\,d\omega, \qquad (5)$$

respectively, with I being the intensity of the monochromatic excitation and $\bar{I}$ the spectral density of broadband excitation. Here and in what follows the homogeneous spectra κ and φ are supposed to be normalized to unity.

For realistic shapes of the homogeneous spectra κ and φ, (4) and (5) cannot be calculated analytically; below we shall present the results of numerical calculations. However, the situation at small burning times $t \ll I_0\sigma\kappa_{\max}\eta$ can easily be analysed. The difference spectra of excitation and fluorescence are given by

$$\Delta I_e(\nu, t) = I_e(\nu, 0) - I_e(\nu, t)$$
$$\approx I_0 I\sigma^2\eta\eta_f t \int_{-\infty}^{\infty} \kappa(\nu-\omega)\,\kappa(\nu_0-\omega)\,\varrho(\omega, 0)\,d\omega \qquad (6)$$

and

$$\Delta I_f(\nu, t) = I_f(\nu, 0) - I_f(\nu, t)$$
$$\approx I_0\bar{I}\sigma^2\eta\eta_f t \int_{-\infty}^{\infty} \varphi(\nu-\omega)\,\kappa(\nu_0-\omega)\,\varrho(\omega, 0)\,d\omega, \qquad (7)$$

respectively.

Omitting the factor $\bar{I}\sigma\eta t$, the right-hand side of (7) coincides with the formula for the selectively-excited fluorescence spectrum, as it is observed in fluorescence line narrowing experiments. The analysis given for this case [53, 54] applies here as well.

Both (6) and (7) contain contributions from burning via NPL and PSB. However, because of the great difference in NPL and PSB peak intensities phonon sideholes become observable only when no-phonon holes (especially the purely electronic one) are already essentially saturated. Note also that for the initial IDF $\varrho(\omega, 0)$, constant in the region of the hole, the excitation spectrum (6) is symmetric even for an asymmetric κ. All information about the asymmetry of κ reveals itself only when the saturation effects become essential (Fig. 3).

For model calculations homogeneous spectra are supposed to consist of narrow NPL κ_0, φ_0 of a Lorentzian shape, and broad PSB κ_p, φ_p of the form

$$\kappa_p(\nu-\omega) = \begin{cases} (1-\alpha)\Gamma_p^{-2}(\nu-\omega)\exp[-(\nu-\omega)/\Gamma_p], & \nu-\omega > 0 \\ 0, & \nu-\omega < 0 \end{cases}$$
$$\varphi_p(\nu-\omega) = \kappa_p(\omega-\nu), \qquad (8)$$

where α is the Debye-Waller factor, and Γ_p characterizes the width of PSB. The evolution of a no-phonon hole in the excitation spectrum is depicted in Fig. 1a. In accordance with (6) the initial hole in the excitation spectrum has also a Lorentzian shape with the width $\delta(0) = 2\Gamma$ (double homogeneous width of the absorption line), and the depth H is proportional to the burning time. In the process of burning the hole broadening takes place and it loses its Lorentzian shape. In the initial stage of burning the ratio of the relative rates of broadening and deepening of the hole is 0.5 for Lorentzian NPL. The time dependence of the hole width δ at small burning times is given by

$$\delta(t) \approx 2\Gamma[1 + \dot{H}(0)t/2I_e^0], \quad H(t) = \Delta I_e(\nu_0, t), \qquad (9)$$

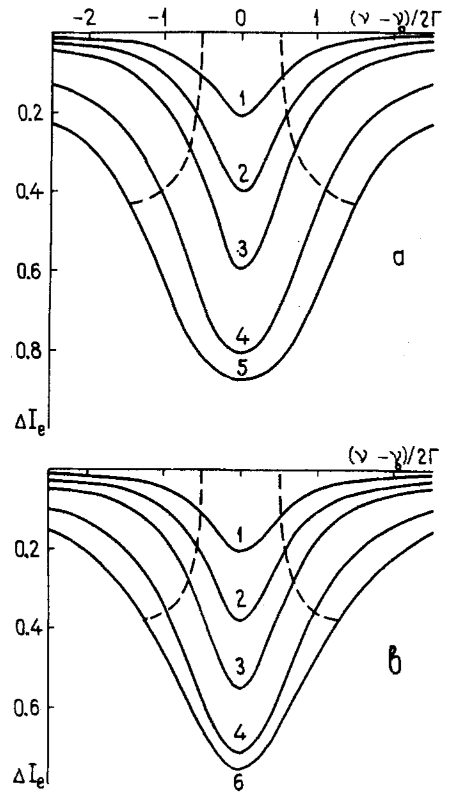

Fig. 1. Evolution of no-phonon hole in the absence (*a*, $W=\infty$) and presence (*b*, $W=15$) of reverse processes. Burning times $t=0.5$ (*1*), 1.2 (*2*), 2.5 (*3*), 9 (*4*), 20 (*5*), and ∞ (*6*) in the units of $\pi\Gamma/2I_0\sigma\eta$

where I_e^0 is the NPL contribution to the initial excitation spectrum. The dependence of the hole width on the depth is given in Fig. 2 (Curve *1*).

The evolution of the phonon sideholes in the excitation (b) and fluorescence (c) spectra is demonstrated in Fig. 3.

1.2. Reverse Processes

The account of reverse processes is essential when the photoproduct is thermally unstable at the burning temperature or when it is photochemically unstable and the photochromic shift is insufficient to avoid the absorption of the burning light. Supposing that the rate of the reverse process is the same for all impurities, the kinetics are then given by

$$\dot{\varrho}(\omega,t) = -K(\omega)\varrho(\omega,t) + \bar{K}[\varrho(\omega,0) - \varrho(\omega,t)]\,, \qquad (10)$$

where

$$K(\omega) = I_0\sigma\eta\kappa(\nu_0-\omega) + K_0 \qquad (11)$$

and

$$\bar{K} = I_0\bar{\sigma}\bar{\eta}\bar{\kappa} + \bar{K}_0\,. \qquad (12)$$

Here K_0 and $\bar{K}_0$ are the rates of direct and reverse thermal reactions, respectively, $\bar{\sigma}\bar{\kappa}$ is the photoproduct

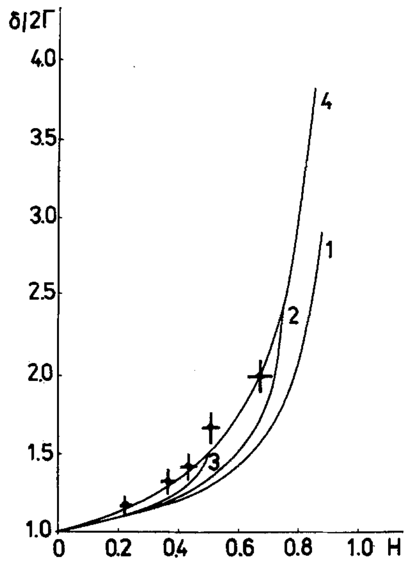

Fig. 2. Dependence of the width of the hole on the depth (in the units of I_e^0) for different relative rates W of reverse processes: $W=\infty$ (absence of reverse processes) (*1*), 15 (*2*), 3 (*3*). Curve *4* corresponds to a saturated hole. Circles represent experimental results for burning in the vibronic band at 14,779 cm^{-1} of H$_2$-tetra-4-tert.-butylphthalocyanine in *n*-nonane at 4.2 K

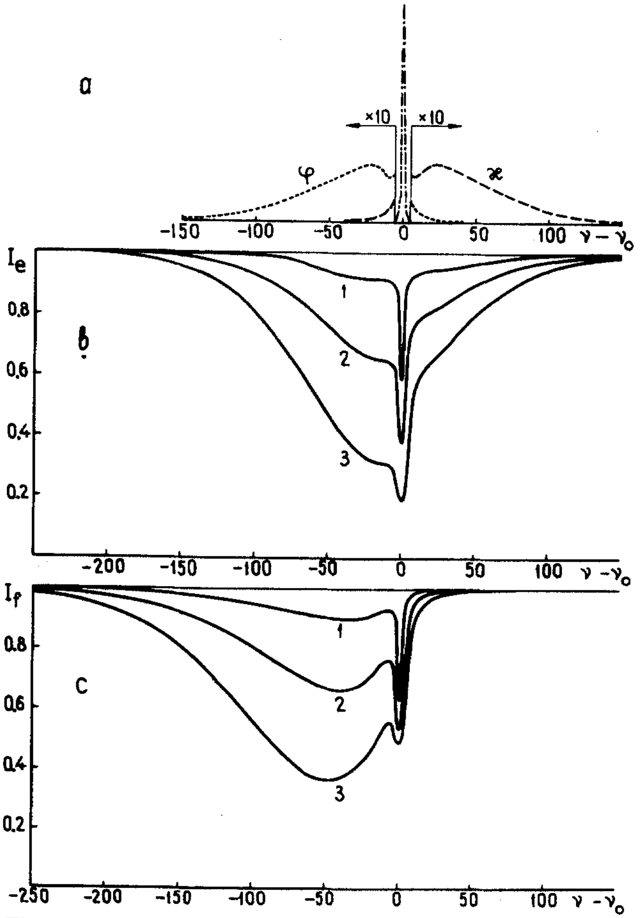

Fig. 3a–c. Evolution of the phonon sidehole in the spectra of excitation (b) and luminescence (c) for model shapes of homogeneous spectra (a). Debye-Waller factor $\alpha=0.5$. PSB width $\Gamma_p=25\Gamma$. Burning times $t=10$ (*1*), 50 (*2*), 150 (*3*) in the units of $\pi\Gamma/2I_0\sigma\eta$

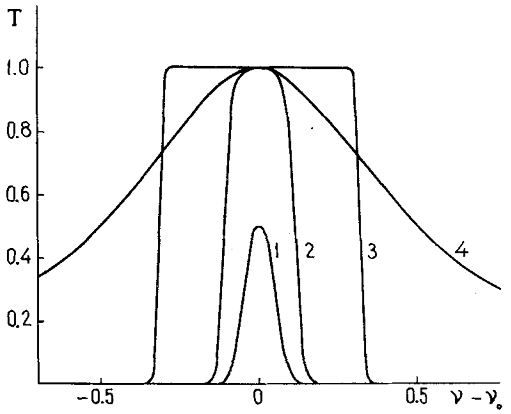

Fig. 4. Hole burning in the transmission spectrum of an optically dense sample with a broad-band light of spectrum 4. The initial density $\ln T(\nu,0)=43.4$ is constant in the actual spectral region. Burning times $t=100$ (*1*), 105 (*2*), 140 (*3*) in the units of $(I_{\max}\sigma\eta)^{-1}$ with $I_{\max}$ being the maximum spectral density of broad-band excitation

absorption cross section at the burning frequency ν_0, and $\bar{\eta}$ is the quantum yield of the reverse photoreaction. Equation (10) applies particularly when the photoproduct absorbs via its broad (compared with the dispersion of photochromic shifts) phonon wings. This is, for example, the case of H_2Pc in Shpol'ski's matrices [55]. For the Lorentzian absorption line the evolution of no-phonon hole is depicted in Fig. 1b. The main effect of reverse processes consists in reaching a stationary shape of a hole at large burning times, which corresponds to the stationary distribution $\varrho(\omega,\infty)$ obtained from (7):

$$\varrho(\omega,\infty)=\varrho(\omega,0)\frac{\bar{K}}{K(\omega)+\bar{K}}. \tag{13}$$

For the Lorentzian absorption line the stationary hole is also Lorentzian with the width

$$\delta(\infty)=\Gamma(1+\sqrt{1+W}), \tag{14}$$

determined by the ratio W of the rates of selectively-excited (via NPL) and non-selective (via PSB and thermal) processes

$$W=\frac{2I_0\sigma\eta/\pi\Gamma}{I_0\bar{\sigma}\bar{\kappa}\bar{\eta}+K_0+\bar{K}_0}. \tag{15}$$

The dependence of the width of the hole on its depth for different values of the parameter W is depicted in Fig. 2 (Curves *2* and *3*). Curve *4*, at which these curves end, corresponds to the satured stationary hole. Note that at equal depths the saturated hole is always broader. Circles in Fig. 2 correspond to the experimental results obtained for free-base tetra-4-tert.-butylphthalocyanine (H_2Pc^*) in *n*-nonane. A comparison with theoretical curves yields for W a value of 8.3, which is determined by the ratio of the vibronic NPL and PSB peak intensities in this system.

1.3. Optically Dense Samples

In the case of optically dense samples the excitation is no longer uniform for all impurities, its intensity depending on their spatial positions and burning time. It can be shown that if the irradiation spectrum $I_0(\nu)$ is much broader than the inhomogeneous absorption lines, the transmission spectrum of the sample, dependent on the burning time t, is given by

$$T(\nu,t)=[(T^{-1}(\nu,0)-1)e^{-I_0(\nu)\sigma\eta t}+1]^{-1}. \tag{16}$$

Here PSB are not taken into account.
For a Lorentzian $I_0(\nu)$ the time evolution of the transmission spectrum is depicted in Fig. 4. Note that the hole width may be less than that of the line used for burning.

1.4. Higher-Dimensional Inhomogeneity

There is a lot of evidence that not only the frequencies of purely electronic transitions but most of the parameters of homogeneous spectra (vibrational frequencies [11], linewidths [56], Debye-Waller factors [41], etc.) are affected by matrix inhomogeneity. In general, only a partial correlation exists between variations of different parameters [57]. To take this into account a higher-dimensional IDF of actual parameters must be introduced. Formulae (4, 5) then include manifold integration over these parameters.
In [12] an inhomogeneous distribution of homogeneous widths uncorrelated with the frequency of purely electronic transition was considered. This leads to a peculiar hole-shape that deviates from the Lorentzian one even in the initial stage of burning.
For the model distribution $\varrho(\omega,\Gamma)=\varrho(\omega)\varrho_\Gamma(\Gamma)$, where

$$\varrho_\Gamma(\Gamma)=\begin{cases}\dfrac{1}{\Gamma_2-\Gamma_1}, & \Gamma_1<\Gamma<\Gamma_2\\ 0, & \Gamma<\Gamma_1, \Gamma>\Gamma_2\end{cases} \tag{17}$$

(Fig. 5a), the resulting hole shape at small burning times is

$$\Delta I_e\sim\ln\frac{\Gamma_2^2+(\nu-\nu_0)^2}{\Gamma_1^2+(\nu-\nu_0)^2} \tag{18}$$

with the width $\delta=2\sqrt{\Gamma_1\Gamma_2}$ (Fig. 5b).
For systems, where one has to take into account the light-induced reverse processes, it is also important to know how the transition frequencies of the initial form of impurity and photoproduct are correlated. A model for describing the hole burning in a system with two

quasistable impurity configurations mutually transformable via photo- or (and) dark processes was proposed in [38], where a phenomenological two-dimensional IDF $\varrho(\omega_1, \omega_2)$ was introduced (ω_1, ω_2 being the transition frequencies in the respective impurity configurations). The form of $\varrho(\omega_1, \omega_2)$ was concretized in [59] for axially symmetric impurities in a cubic lattice, where photoinduced transitions between different geometrically equivalent impurity orientations occur (e.g., O_2^--type molecular ions in alkali halids [60]). In Fig. 6 results of these calculations are depicted, which demonstrate the existence of only a partial correlation between transition frequencies in different orientations of the impurity.

1.5. Impurity-Impurity Interactions

To consider PHB in samples with high impurity concentration it is necessary to take into account impurity-impurity interactions. The influence of energy transfer on selectively-excited luminescence spectra was considered in [61]. It can be applied to the hole spectra in the initial stage of burning as well. Another possible but less apparent effect of impurity-impurity interactions on PHB was considered in [59]. The burning out of a part of impurities is effectively equivalent to the creation of new defects for the remaining ones. The new defects act as a new source of inhomogeneous broadening. Considering impurities as interacting elastic dipoles an equation was derived to describe such a process:

$$\frac{\partial\varrho}{\partial t} = -\Delta BQ\frac{\partial\varrho}{\partial\omega} - \frac{|\Delta A|}{\pi}Q\frac{\partial}{\partial\omega}\mathscr{P}\int_{-\infty}^{\infty}\frac{\varrho(\omega')}{\omega-\omega'}d\omega' - K\varrho, \qquad (19)$$

where

$$Q = \int_{-\infty}^{\infty} K(\omega)\,\varrho(\omega,t)\,d\omega,$$

and

$$K(\omega) = I_0\sigma\eta\kappa(\nu_0-\omega).$$

ΔA, ΔB in (19) are proportional to the change of the elastic momentum of an impurity in the photochemical reaction. The effect of such quasi-static impurity-impurity interactions is to increase the relative rate of hole-broadening and to shift the hole maximum from the burning frequency. Particularly, when photoactive impurities themselves are the sole source of inhomogeneous broadening, (9) is modified to

$$\delta(t) \approx 2\Gamma[1+(0.5+|\Delta A/A|)\,\dot{H}(0)\,t/I_e^0]. \qquad (20)$$

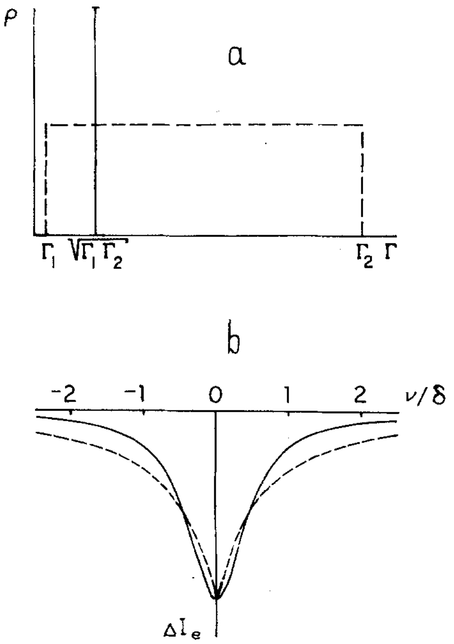

Fig. 5. Model distribution of homogeneous linewidth Γ (*a*, dashed curve, $\Gamma_2/\Gamma_1 = 30$) and the respective hole contour at small burning times (*b*, dashed curve) compared to a Lorentzian hole (*b*, solid curve) of the same width $\sigma = 2\sqrt{\Gamma_1\Gamma_2}$

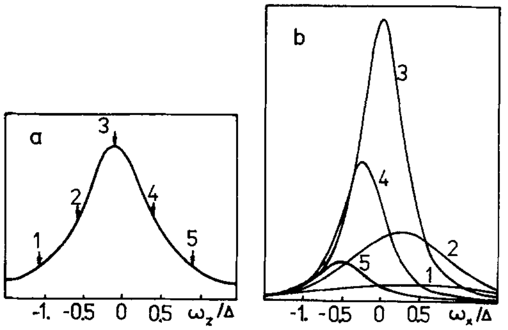

Fig. 6a and b. Inhomogeneous distribution of transition frequencies ω_z in an orientation of axially symmetric impurities, fixed along a certain C_4-axis of a cubic crystal (a) and frequency distributions after a 90°-reorientation for fixed values of the initial frequency (b). Curves *1*–*5* correspond to arrows *1*–*5* in (a)

Such hole-broadening may be remarkably effective if a large number of holes is burned into a inhomogeneous spectrum.

1.6. Effects of Hole-Burning in Fluorescence Line Narrowing

Photochemical processes can also essentially affect selectively-excited luminescence spectra. Particularly, a redistribution of intensities between NPL and the sideband during the excitation has been observed in several systems [25, 62]. This results from different

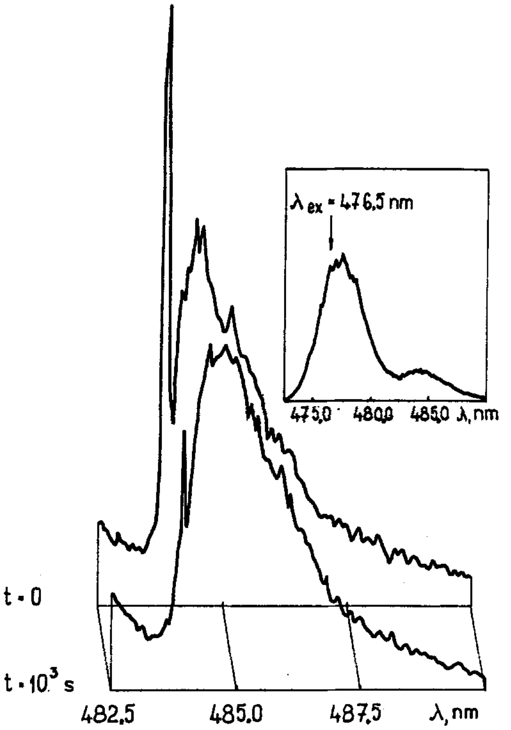

Fig. 7. Selectively-excited luminescence spectra of tetracene in a glassy matrix at different excitation times at 4.2 K. Inset represents the inhomogeneously-broadened luminescence spectrum (0–0 band and its 310 cm^{-1} replica); the position of selective (laser) excitation is indicated

burning rates at an excitation in NPL and PSB (Fig. 7). In this case the ratio of NPL and sideband integral intensities observed in selectively excited spectra does not correspond to the Debye-Waller factor. This may result in an unusual temperature dependence – an increase with temperature – of NPL relative intensities in a selectively excited spectrum. For a model accounting for light-induced redistributions between different conformations of photoactive impurities, it was demonstrated that the relative NPL intensity may under some conditions be proportional to $\Gamma(T)$ [63]. A similar dependence – an increase with temperature – was qualitatively proposed to occur also in the transient regime of the basic model [62].

2. PHB Application to Problems of Molecular Spectroscopy

2.1. Homogeneous Linewidth of Pure-Electronic Transition and its Temperature Dependence

PHB was used to obtain the HLW of the pure-electronic $S_1 \leftrightarrow S_0$ transition of H_2Pc^* in crystalline *n*-tetradecane (H_2Pc^*–C_{14}) [10, 42, 43]. The pure-electronic multiplet consists of two intensive lines related by a photochemical transformation (see Sect. 2.5), and of a few weak ones. An irradiation at a Ne-discharge line of 692.947 nm (0.08 cm^{-1} width) created a hole in the inhomogeneously-broadened component at 693.0 nm. The HLW was determiend as the zero-time limit of the hole width $\delta(t)$ created at different irradiation times. As it follows from (9) after correcting for the instrumental width, this yields the limiting hole width of 2Γ. At temperatures of $6 \div 30$ K holes were detected in luminescence at instrumental widths of 0.1 and 0.26 cm^{-1}. An additional monochromatization with the RC-110 Fabry-Perot interferometer (instrumental widths 0.0027 and 0.0055 cm^{-1}) was used for burning at lower temperatures ($1.8 \div 8$ K), and holes were measured in the excitation spectra by scanning the same interferometer across the discharge line contour. Luminescence was integrally recorded at $\lambda > 710$ nm.

Data on $\Gamma(T)$ obtained from two sets of experiments are depicted in Fig. 8. At 1.8 K the pure electronic NPL was found to be very narrow with $\Gamma = 0.002 \pm 0.0008\ \mathrm{cm}^{-1}$. The contribution of population-decay processes to this value was obtained from the fluorescence decay measurements: $T_1 = 5.2$ ns at 4.2 K and 5.5 ns at 77 K, i.e. it is practically temperature independent in the region of interest. Taking $\Gamma^{\|} = 1/T_1 = 0.001\ \mathrm{cm}^{-1}$ as constant, one can extract the contribution to the HLW thanks to a phase relaxation process $\Gamma^{\perp}(T)$. The dephasing broadening at 1.8 K is then $\Gamma^{\perp} = 2/T_2' = 0.001\ \mathrm{cm}^{-1}$ and the corresponding dephasing time $T_2' = 10$ ns. The experimental data for $\Gamma^{\perp}(T)$ are presented in Fig. 8b logarithmically together with the theoretical curves describing the dependence of the phonon-induced dephasing rate on temperature. A theoretical approach to the contribution of pure dephasing processes to the HLW [64, 36] was based on a quadratic electron-phonon coupling and harmonic phonon approximation. It leads to the effect of Raman scattering of phonons. At low temperatures, when the density of phonon states can be approximated by the Debye distribution, the dephasing broadening is given by Curve *1*. Here the characteristic Debye temperature T_D is taken 50 K, as follows from the phonon spectra of *n*-alkanes [2]. Curve *1* fits the experimental data only at high temperatures ($T \gtrsim T_D$). In the high-temperature limit the simple T^2-dependence should be theoretically observed. It can be seen that such a quadratic temperature dependence is in good accordance with the experimental dots at temperatures $10\,\mathrm{K} \lesssim T \lesssim T_D$. At $T < 10$ K $\Gamma(T)$ decreases approximately as T^4. All experimental data can be described taking into account one kind of phonons only, presumably pseudolocalized phonons of frequency ω_0 [65]. For this simple single-mode case $\Gamma^{\perp}(T)$ is expressed as follows:

$$\Gamma^{\perp} = b\bar{n}(\omega_0)\,[\bar{n}(\omega_0) + 1]\,,$$

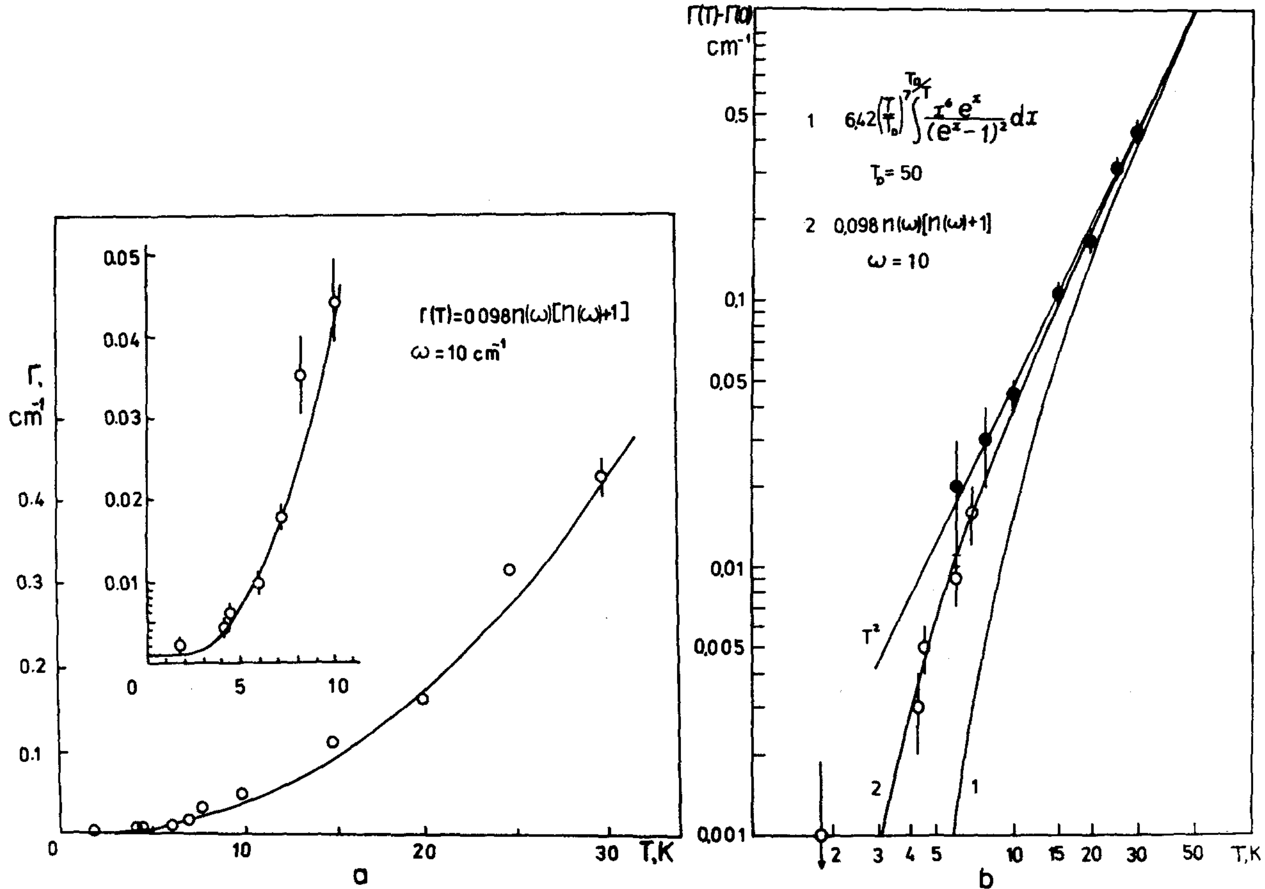

Fig. 8a and b. HLW temperature dependence for pure-electronic transition in H_2Pc^*–C_{14} in an ordinary (a) and a double-logarithmic (b) plot. Curves *1* and *2* are calculated using

$$6.42(T/T_D)^7 \int_0^{T_D/T} x^6 e^x (e^x-1)^{-2}\,dx \quad \text{with} \quad T_D = 50\,\mathrm{K} \quad \text{and} \tag{1}$$

$$0.098\, n(\omega)\,[n(\omega)+1] \qquad \text{with} \quad \omega = 10\,\mathrm{cm}^{-1} \tag{2}$$

where

$$\bar{n}(\omega_0) = \left(e^{\frac{\hbar\omega_0}{kT}} - 1\right)^{-1}. \tag{20}$$

For a approximation (Curve *2*) we take the parameters $\omega_0 = 8 \div 12\,\mathrm{cm}^{-1}$ and $b = 0.06 \div 0.19\,\mathrm{cm}^{-1}$. The calculated total HLW $\Gamma(T)$ is presented in Fig. 8a by a solid line. Its limit at $T = 0$ coincides with Γ^{II} within experimental errors.

The indicated variation in the values of the parameters ω_0 and b is not large, and it permits to estimate the frequency of the pseudolocalized mode and the quadratic electron-phonon coupling constant. At the frequency $2\omega_0 = 20\,\mathrm{cm}^{-1}$ a maximum in the phonon wing was observed in the phonon sidehole and in the excitation spectrum of the system, that may serve as additional evidence of the low-symmetry pseudolocal vibration, which is inactive in the allowed electronic transition. This vibration may be some vibrational mode of the impurity molecule carrying, evidently, the most part of the quadratic electron-phonon coupling. So, no interaction with the regular phonons in the low-temperature region of low phonon density appears experimentally.

2.2. *Homogeneous Linewidth in Glasses*

Recently there was some evidence that the HLW of some optical transitions in rare-earth ions in inorganic glasses are anomalously broad, and reveal a quadratic dependence on temperature at low temperatures [66]. This was shown to be consistent with a model developed by Lyo and Orbach [67] involving an interaction of the optical transition with disorder modes which are known to exist in amorphous systems [68]. We have applied PHB in order to compare HLW and its temperature dependence for the $S_0 - S_1$ transition of H_2Pc^* in organic glass (GL, 2:5 isopropanol/ether mixture) in crystalline matrices (*n*-nonane C_9 and tetradecane C_{14}) [25, 43]. An oxazine dye laser was used as a tunable irradiation source in the above

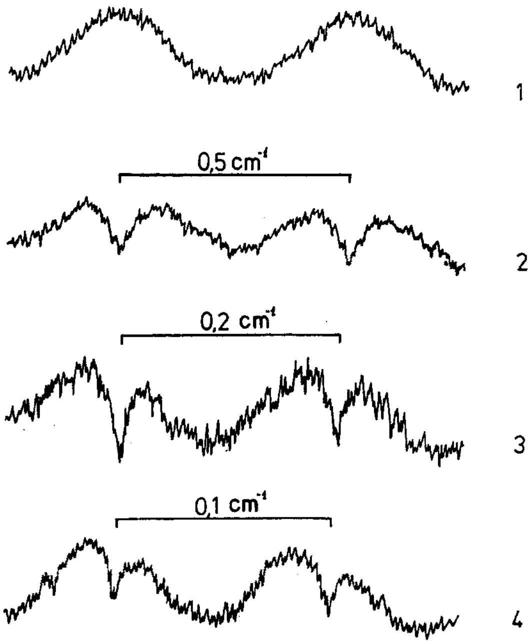

Fig. 9. Hole in the excitation spectrum of H_2Pc^* in different matrices at $T=1.8$ K. (*1* initial spectrum before burning, *2* glassy matrix, *3* *n*-nonane, *4* tetradecane)

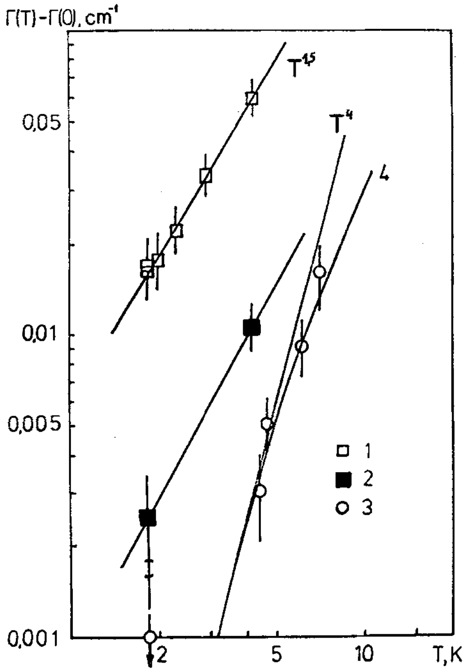

Fig. 10. HLW temperature dependence for purely electronic transition in H_2Pc^* in *1* glass, *2* *n*-nonane and *3* tetradecane. Curve *4* coincides Curve *2* in Fig. 8

experimental setup. The irradiation intensities were attenuated by 40 times at switching-over from burning to recording, which made possible distortionless hole-contour measurements. It was shown that the holes in the spectra of H_2Pc^* are dependent on matrices (Fig. 9). The holes were the broadest in GL, where IHB was large (170 cm^{-1}), and narrowest in C_{14} (Spol'skii matrix). In crystalline C_9, where IHB was about as large as in GL, the holes were of intermediate width. HLW at 1.8 K were 0.017, 0.0035, and 0.002 cm^{-1} in GL, C_9, and C_{14}, respectively, which demonstrates an essential role of the matrix structure. The HLW temperature dependence for the three matrices is shown in Fig. 10. Rather a slow broadening was observed for the glassy matrix. The best fit with $T^{1.5\pm0.3}$ is slower than that obtained for inorganic systems [66, 67]. The observed features in glasses do not qualitatively contradict the ordinary broadening by phonon-induced Raman dephasing processes with the account of the increased density of low-frequency disorder modes [67, 69].

Because of a rather large time interval between the creation of a hole and its recording a temporal broadening due to the rearrangement of the impurity surrounding in a glassy matrix is also possible. However, no temporal changes in the hole width were observed when the time of the burning-recording cycle was varied from 10^2 to 10^{-2} s. Supposing that the anomalous hole width in glasses is determined by the transition frequency fluctuation [70], the hole width yields an estimate for the amplitude of these fluctuations, which is equal to 0.05 cm^{-1}, while the lower limit for the characteristic time of fluctuations is 10^{-2} s.

An anomalously large hole width in the spectra of aromatic molecules such as perilene, tetracene, etc. [26, 28], obtained by NPHB in glassy matrices, can probably be explained by the above-considered mechanisms.

A high degree of the structural disorder of glassy matrices is expected to affect not only transition energies but other parameters of homogeneous spectra as well resulting in a higher-dimensional inhomogeneity, see (1.4), which may reshape, in particular, hole contours, see (18).

For a precise measurement of hole contours a single-frequency dye laser CR-699-21 on rhodamine B, providing a spectral width of about 3 MHz, was used [12]. Holes were burned in the spectra of H_2-tetra(tert.-butyl)porphirazine (TAP*) in GL and *n*-hexane (C_6). Inhomogeneous electronic bands in these matrices are structureless, with the widths of 170 and 120 cm^{-1}, and they are located at 617 and 619 nm, respectively. The hole contours at 1.8 K are shown in Fig. 11 where the dots represent the Lorentzian approximations. The hole is Lorentzian in C_6 with $\Gamma=0.005$ cm^{-1}.

A specific hole shape was observed in GL, which appears to be Lorentzian in the upper part and reveals rather a slow decrease in the wings. This hole shape was interpreted as a result of the dispersion of the values of Γ. From a comparison with model calcu-

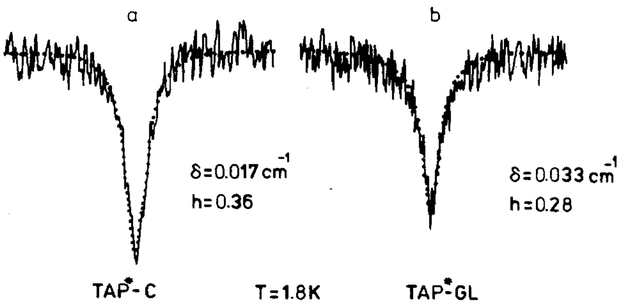

Fig. 11. Holes in the excitation spectra of TAP*–C_6, $\lambda_{ex}=619.7$ nm (a) and TAP*–GL, $\lambda_{ex}=618.3$ nm (b), obtained by 30-fold storage. Burning intensity and time are $2\,\mu W\,cm^{-2}$ and 0.3 s, respectively, $T=1.8$ K

lation (Fig. 5) the ratio $\Gamma_{max}/\Gamma_{min}$ for the centres with coincident electronic transition frequencies was estimated to be $8 \div 10$. In this way the hole contour is formed by the HLW $0.005 \leqq \Gamma \leqq 0.05\,cm^{-1}$. It is interesting to note that the lower limit of Γ in GL coincides with that for C_6, indicating the existence of impurities interacting weakly with the disorder modes of a glassy matrix.

2.3. *Homogeneous Linewidth of the Vibronic Transition*

At vibronic transitions PHB enables one to determine the homogeneous widths of vibronic NPL, times and mechanisms of vibrational relaxation. We consider here the temperature broadening of vibronic NPL in H_2Pc^*–C_9 at $\nu_{00}+515\,cm^{-1}$ [47]. The data obtained by PHB for temperatures of 1.8–60 K are presented in Fig. 12. The temperature dependence of HLW fits well with the approximation $\Gamma_{01}(T)=\Gamma(0)+aT^{2.4\pm0.2}$. An extrapolation to zero temperature gives $\Gamma_{01}(0)=2.8\,cm^{-1}$ yielding the lifetime of the $515\,cm^{-1}$ local vibration, $T_1=1.9$ ps. It is natural to suppose that the decay of an internal vibration in an impurity molecule is caused by anharmonic interactions with crystalline phonons and other molecular vibrations.

The scheme of the lower vibronic levels of the H_2Pc^* molecule allows one to discuss the possible ways of energy relaxation. There are two channels of anharmonic decay which involve only one crystal phonon: (a) transition to the nearby $441\,cm^{-1}$ level with the creation of the $74\,cm^{-1}$ phonon ($515=441+74$) and (b) transition to the higher $563\,cm^{-1}$ level with the annihilation of the $48\,cm^{-1}$ phonon ($515=563-48$). The calculated temperature dependences of the respective decay probabilities are shown in Fig. 12. Curve *1* corresponds to the decay channel (a); Curve *2* results from the contributions of both channels, (a) and (b), supposing equal anharmonic coupling constants for the 441 and $563\,cm^{-1}$ vibrations. Both curves demonstrate a weak dependence of the decay probability on temperature at $T<60$ K due to a rather high frequency of phonons involved. It is obvious that, in addition to (a) and (b), a dephasing process which is of the same order of probability as the two-phonon decay, should also be taken into account. Since there are many possible combinations of phonons and local vibrations bringing about such processes, we incorporate the broadening by two-phonon Raman scattering only. Curve *3* summarizes the broadening of vibronic transitions by the anharmonic decay processes (a)+(b) and by a single-mode dephasing due to the scattering of the pseudolocal vibration of frequency, $20\,cm^{-1}$. Curve *3* gives a rather good approximation for the HLW measured at $T<50$ K. The deviations at $T>50$ K indicate that other crystalline and molecular vibrations should be accounted.

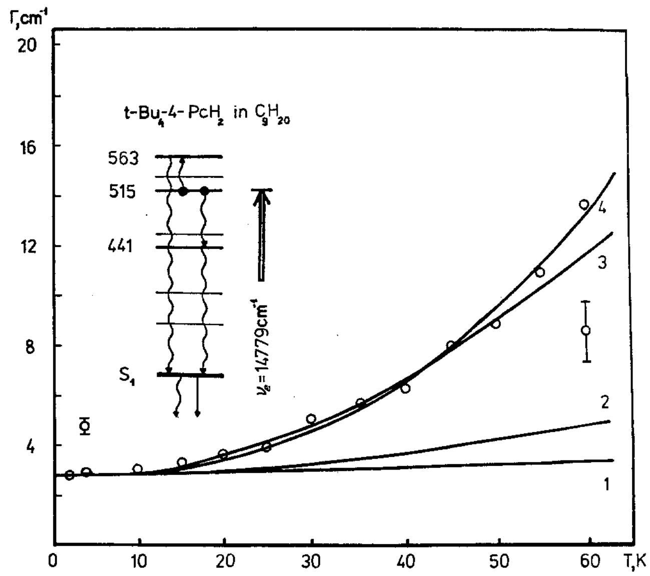

Fig. 12. HLW temperature dependence for $\nu_{00}+515\,cm^{-1}$ vibronic transition in H_2Pc^*–C_9. Curves are calculated using

$$\Gamma(T)=2.8[n(\omega_1)+1], \qquad \omega_1=74\,cm^{-1} \tag{1}$$

$$\Gamma(T)=2.8[n(\omega_1)+1]+2.8n(\omega_2), \quad \omega_2=48\,cm^{-1} \tag{2}$$

$$\Gamma(T)=2.8[n(\omega_1)+1]+2.8n(\omega_2) + 1.5[n(\omega_3)+1]n(\omega_3), \quad \omega_3=20\,cm^{-1} \tag{3}$$

$$\Gamma(T)=2.8+0.56\times10^{-3}\cdot T^{2.4}, \tag{4}$$

respectively. In the left inset a scheme of actual vibronic levels is depicted, demonstrating the most probable decay channels of $\nu_{00}+515\,cm^{-1}$ vibronic state

2.4. *Inhomogeneous Broadening of Local Vibrations*

In this section impurity molecules with a fixed frequency of the pure-electronic (ν_{00}) or the vibronic (ν_{01}) transition will be shown to reveal an inhomogeneous distribution of frequencies of the internal vibration Ω [11]. The width of this distribution K (K' when ν_{01} is fixed) can be measured when comparing the widths of the hole burned directly at ν_{00}, and a hole replica at

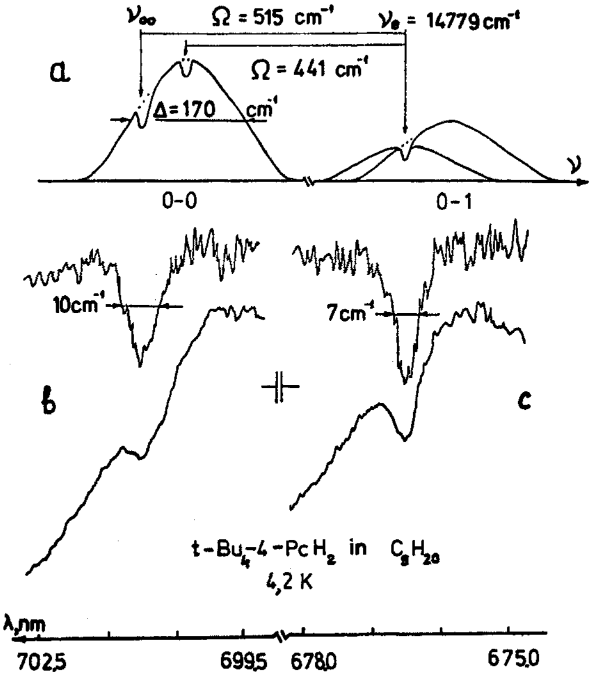

Fig. 13a–c. Schematic absorption spectrum demonstrating hole burning in the vibronic (0–1) band (a). Excitation spectra in the vicinity of $\nu_{00} = \nu_0 - 515\,\mathrm{cm}^{-1}$ (b) and $\nu_{01} = \nu_0$ (c) after burning in the vibronic 0–1 band with 676.44 nm laser line. Luminescence is recorded at 736.5 nm (b) and 700.9 nm (c). Upper curves demonstrate hole contours obtained by subtracting the lower spectra from the initial ones

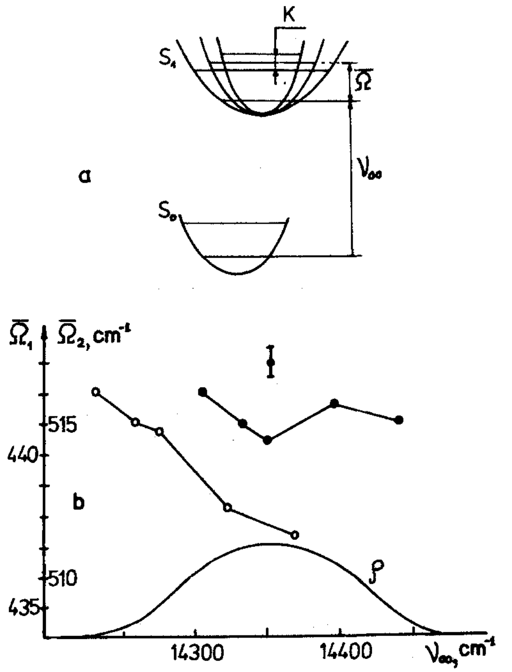

Fig. 14. (a) Origin of vibrational inhomogeneity: fixation of purely electronic transition frequency does not fix the intramolecular vibration frequency. (b) Variation of the mean frequency of 441 cm⁻¹ ($\bar{\Omega}_1$, solid circles) and 515 cm⁻¹ ($\bar{\Omega}_2$, hollow circles). Lower the IDF is depicted

$\nu_{00} + \Omega$ (Case a) or when a hole is burned directly at ν_{01} and has its replica at $\nu_{01} - \Omega$ (Case b). The multiplication of holes is explained by the scheme in Fig. 13. Supposing Lorentzian shapes for the distribution of vibrational frequencies and homogeneous lines, simple formulae may be obtained for the respective hole widths

$$\delta_{00} = 2\Gamma_{00},\ \delta_{01} = \Gamma_{00} + \Gamma_{01} + K\,; \tag{21}$$

in the case (a) and

$$\delta'_{00} = \Gamma_{00} + \Gamma_{01} + K',\ \delta'_{01} = 2\Gamma_{01}\,, \tag{22}$$

in the Case (b).

Experiments were performed on H_2Pc^*–C_9 by burning in the vibronic band at $\nu_{01} = \nu_{00} + 515\,\mathrm{cm}^{-1}$ (Case b) with a crypton laser line. The holes and their replicas are shown in Fig. 13. The hole widths δ'_{01} and δ'_{00} were found to be 8 and 10 cm⁻¹, respectively. Neglecting Γ_{00} and taking into account the instrumental width of 1 cm⁻¹ one obtains $K' = 5.8 \pm 0.5\,\mathrm{cm}^{-1}$. When the experimental scheme (a) was realized, it yielded $K = 6.3 \pm 1\,\mathrm{cm}^{-1}$.

For the vibrational IDF of a Gaussian shape one obtains $K \approx K' \approx 8\,\mathrm{cm}^{-1}$. Hence, monochromatic excitation in the 0–0 region fixes the energy difference between the adiabatic potentials of the ground and excited states and does not fix their curvatures, see Fig. 14a.

It is interesting to compare the variation of molecular vibrational frequencies for the molecules with the same and with different energies of the electronic transition. The latter value $\Delta\bar{\Omega}$ was obtained from the positions of the vibronic NPL in luminescence measured at selective excitation within the inhomogeneous band. The results of these experiments are depicted in Fig. 14. For the 515 cm⁻¹ vibration a monotonous decrease of $\bar{\Omega}$ with the increase of ν_{00} was observed, with the variation $\Delta\bar{\Omega} = 5\,\mathrm{cm}^{-1}$, i.e. of the order of K.

For the 515 cm⁻¹ vibration the relative magnitudes of both the inhomogeneous vibrational dispersion $K/\bar{\Omega}$ and the vibrational frequency variation $\Delta\bar{\Omega}/\bar{\Omega}$ are close to the relative value of the electronic frequencies: $K/\bar{\Omega} \approx \Delta\bar{\Omega}/\bar{\Omega} \approx \Omega/\nu_{00} \approx 1\%$. This indicates that vibrations may be as sensitive to the inhomogeneity of matrix as the electronic transition is. For the 441 cm⁻¹ vibration the variation of the mean $\bar{\Omega}$ within the inhomogeneous band is smaller: $\Delta\bar{\Omega} = 1\,\mathrm{cm}^{-1}$. The respective width of the inhomogeneous vibrational distribution is also substantially smaller, which indicates the different influence of matrix imperfections on different impurity vibrations.

From the fact that the vibrational inhomogeneity is not small relative to the HLW Γ_{01} an important conclusion follows that inhomogeneous broadening

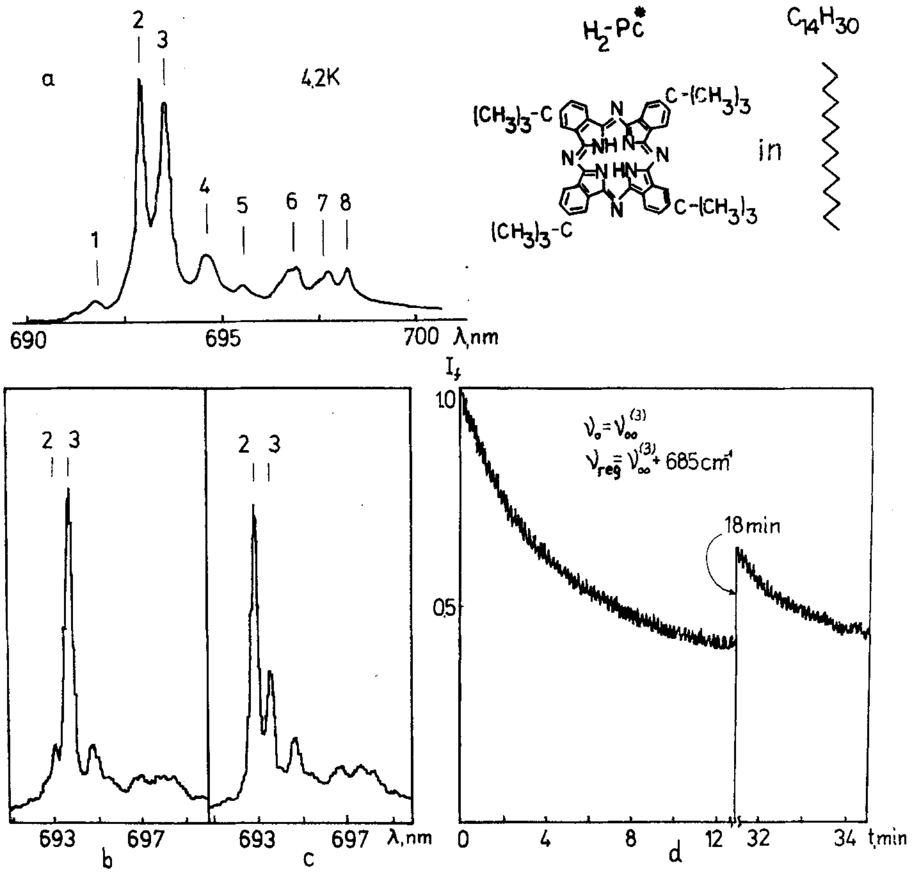

Fig. 15. (a)–(c) Luminescence spectra in the region of the 0–0 multiplet of H_2Pc^*–C_{14} at excitation with $\lambda = 654$ nm, $\Delta\lambda = 4$ nm before (a) and after (b) and (c) selective ($\Delta\lambda = 0.4$ nm) irradiation in components 2 (b) and 3 (c). (d) Temporal dependence of the intensity of component 3 in the luminescence spectrum, registered in the vibronic band at $\nu_{00} - 685\,\mathrm{cm}^{-1}$. Dark pause of 18 min is indicated

can be completely eliminated by a resonant excitation only. Experiments on the laser excitation of luminescence [71, 72] give us only the upper estimate of HLW of vibronic transitions.

Additional distribution of vibrational frequencies prevents the total elimination of inhomogeneous broadening by a non-resonant monochromatic excitation.

2.5. Investigation of Photochemical Reactions by PHB

The nature of phototransformations in free-base porphyrins is now well-known as the result of a pairwise displacement of inner hydrogens in the centre of the tetrapyrrole ring [73] but the detailed mechanism of the process has not yet been established. Because of the low symmetry of the impurity molecule environment in the crystal matrix two rotational tautomers in a crystal have different energies of local electronic states and different transition frequencies, which brings about the appearance of two components in optical spectra. Figure 15a shows the multiplet of the 0–0 transition of H_2Pc^* in C_{14} at 4.2 K. Two intense components, 2 and 3, undergo mutual transformation under selective photoexcitation (Fig. 15b and c), demonstrating that they belong to the two tautomers. The dependence of the phototransformation rate on excitation intensity was estimated to be linear, while the quantum yield of the one-step photochemistry was obtained to be 10^{-3}. A dark process was found to go from the tautomer in site 2 to that in site 3 at the rate of $\tau^{-1} = 0.5 \times 10^{-3}\,\mathrm{s}^{-1}$. This is well observed by the kinetic curves in Fig. 15d. Since the tautomer in site 3 turns out to be stable in darkness, its energy in the electronic S_0 state should be lower than that in site 2. For the H_2Pc molecule in C_8 analogous phototransformation processes were found [51] but both tautomers were stable in darkness up to 77 K, indicating a high potential barrier between the two minima of the S_0 state. This permits us to study the temperature dependence of phototransformation rates and to exclude one possible pathway of the reaction, viz. over electronic S_1 state. A possible mechanism of phototransformation for H_2Pc and H_2Pc^* molecules may be the vibronic mixing of T_2 and T_1 states, as was proposed by Voelker and van der Waals for free-base porphyn [5].

Phototransformations of the Tetracene Molecule in Crystals and Glasses. In connection with the recent discussion on mechanisms of NPHB in the spectra of photochemically stable molecules in glassy matrices [28] we studied the kinetics of hole burning in the spectra of tetracene in crystalline (n-hexadecane) and

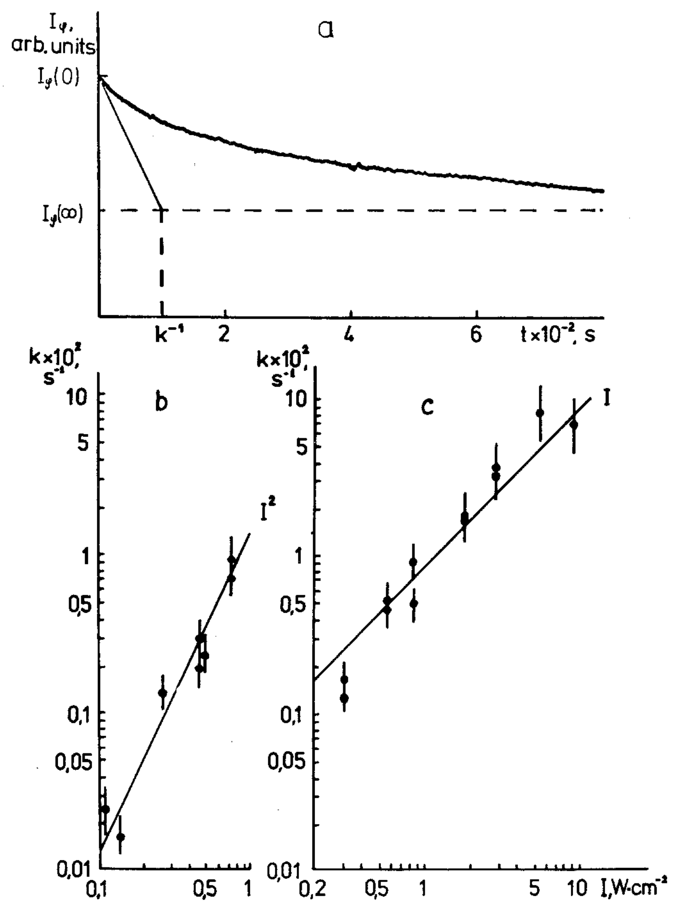

Fig. 16. (a) Temporal dependence of the luminescence intensity of tetracene in a glassy matrix, registered in the vibronic band at $\nu_{00}-310\,\mathrm{cm}^{-1}$, $\lambda_{\mathrm{ex}}=476.5\,\mathrm{nm}$, $J=0.7\,\mathrm{W/cm}^2$. (b) and (c) Dependences of the burning rate on irradiation intensity in glassy (b) and crystalline (c) matrices

glassy (2 : 5 volume fractions isopropanol – ether mixture) matrices [25]. In both systems the inhomogeneous distribution is broad and structureless. For hole burning a 476.5 nm Ar-laser line was used in resonance with the 0–0 band of the S_0-S_1 transition. A temporal decrease of the luminescence signal registered at NPL of the $310\,\mathrm{cm}^{-1}$ vibronic replica was observed in both matrices. An example of the kinetic curve is represented in Fig. 16a.

The burning rate was determined as the initial relative slope of the kinetic curve

$$k=I_{\varphi}^{-1}\left.\frac{dI_{\varphi}}{dt}\right|_{t=0}.$$

In a crystal the burning rate reveals a linear dependence on the excitation intensity $k\sim I$. This indicates the one-step nature of the burning process whose detailed mechanism, however is, not clear yet.

An estimation of the phototransformation quantum yield gave a rather small value, namely $\sim 10^{-8}$. A spontaneous thermal hole filling in darkness was also observed. These are probably the reasons why such phototransformations of tetracene had not been observed earlier [28].

In a glassy matrix a quadratic dependence of the burning rate on the excitation intensity $k\sim I^2$ was observed, indicating a two-step nature of the process. This process goes evidently via higher excited states with the absorption of an additional photon in the photoexcited S_1 or T_1 state. The difference between the observed crystalline and glassy matrices can be explained (a) by a lower ionization threshold of our glass in comparison with that of hexadecane and/or (b) by a more rapid diffusion of photoreaction products in a less rigid glassy matrix, which avoids recombination. Further investigations are needed to clear up definite reaction channels.

2.6. PHB in Spectra of Chlorophyll-Like Molecules

Hole burning in the spectra of chlorophyll and some of its closest derivatives has recently been performed [20–22]. A triplet state bottle-neck hole burning was observed in the spectrum of chlorophyll-*a* (Chl-*a*) [20] and protochlorophyll (PChl) [21] in ether solutions at 4.2 K. The hole of this type was filled in accordance with the triplet state lifetime.

Apart from the fast processes caused by the build-up and decay of the triplet state, slow hole burning processes were found in the spectrum of PChl [22]. These processes, called site interconversion, cannot be explained as hydrogen tautomeric transitions, because in PChl two hydrogen atoms are replaced by a magnesium atom. The same mechanism was found to be mainly responsible for the hole burning in Chl-*a* [21]. A value of $0.01\,\mathrm{cm}^{-1}$ for the width of the hole at 1.8 K was obtained. Holes were stable in darkness at 4.2 K. Site interconversions may be assigned to changes in the strength of the ligation to magnesium as well as to some peripheral groups.

A process similar to the hydrogen tautomeric transition was found in metal-free Chl-*a*, i.e. pheophytin-*a* [21]. In this molecule the two possible orientations of the inner hydrogen pair are not equivalent, that causes quite a large shift (about $500\,\mathrm{cm}^{-1}$) of the 0–0 band of the new phototautomer. The fluorescence excitation spectrum was measured and narrow ($\approx 0.15\,\mathrm{cm}^{-1}$ at 4.2 K) holes were burned in the 0–0 band of the new photoproduct. For the formation of the phototautomer a yield of 10^{-3} was obtained. The lifetime of the S_1 state of the phototautomer was measured to be 4.4 ns, while that of Pheo-*a* was 7.9 ns.

Since reversible photochemistry is a primary step in photosynthesis, the investigation of photochemical processes in vitro by the hole burning seems to be especially interesting.

3. Concluding Remarks

The theoretical and experimental results presented in this paper attempt to demonstrate the ample possibilities of the photochemical hole burning technique. The burning of narrow spectral holes in inhomogeneously-broadened optical bands is based on the use of the inherent properties of an impurity molecule in solids, such as the existence of narrow no-phonon lines in low-temperature spectra and the instability of the molecule in an excited electronic state. This suggests a large number of systems for the possible application of the method as well as indicates its limitations. We have demonstrated the possibilities of applying the hole burning to the spectral investigations of large molecules with a complex level structure, which are otherwise limited by the inhomogeneity of the systems.

The most interesting results seem to be the experimental measurements of the microscopic origin of dephasing and vibrational relaxation processes. In the case of complex organic molecules this method will supply a simple probe of nonradiative relaxation. A comparison with the corresponding results obtained by the methods of transient coherent laser spectroscopy might reveal some interesting new aspects of the problem.

An additional examination of hole formation kinetics in glassy matrices is probably needed to clarify the existence of specific non-photochemical mechanisms of phototransformations in glasses.

The experimental study of energy transfer and the Anderson energy localization in crystals and disordered solids by the hole burning is also an important field requiring further examination.

Some of the possible technical applications of the hole burning method have to be noted. Hole burning can be applied in building computer memory devices with high storage density [74]. Optical filters with a very narrow optical bandpass or with a desired bandpass profile can also be designed.

Acknowledgement. The authors are indebted to V. S. Letokhov for the proposal to write the article.

References

1. R.I. Personov, E.I. Al'shits, L.A. Bykovskaya: Opt. Commun. **6**, 169 (1972)
2. R.I. Personov: In *Molecular Spectroscopy*, a series in Modern Problems in Solid State Physics, ed. by V. M. Agranovich and R. M. Hochstrasser (North-Holland, Amsterdam 1981)
3. L.A. Rebane: Zh. Prikl. Spektrosk. **34**, 1023 (1981)
4. A.A. Gorokhovskii, R.K. Kaarli, L.A. Rebane: JETP Lett. **20**, 216 (1974); Opt. Commun. **16**, 282 (1976)
5. S. Voelker, J.H. van der Waals: Mol. Phys. **32**, 1703 (1976)
6. S. Voelker, R.M. Macfarlane: Mol. Cryst. Liq. Cryst. **50**, 213 (1979); IBM J. Res. Dev. **23**, 547 (1979); J. Chem. Phys. **73**, 4476 (1980)
7. A.I.M. Dicker, J. Dobkowski, S. Voelker: Chem. Phys. Lett. **84**, 415 (1981)
8. H. de Vries, D.A. Wiersma: Phys. Rev. Lett. **36**, 91 (1976)
9. H. de Vries, D.A. Wiersma: Chem. Phys. Lett. **51**, 565 (1977)
10. A.A. Gorokhovskii, L.A. Rebane: Opt. Commun. **20**, 144 (1977)
11. A.A. Gorokhovskii, J.V. Kikas: Opt. Commun. **21**, 272 (1977)
12. A.A. Gorokhovskii, J.V. Kikas, V.V. Palm, L.A. Rebane: Izv. Akad. Nauk SSSR, Ser. Fiz. (1982) in press
13. A.P. Marchetti, M. Scozzafava, R.H. Joung: Chem. Phys. Lett. **51**, 424 (1977)
14. V.G. Maslov: Opt. Spektrosk. **43**, 388 (1977); **45**, 824 (1978)
15. F. Graff, H.-K. Hong, A. Nazzals, D. Haarer: Chem. Phys. Lett. **59**, 217 (1978)
16. F. Düssler, F. Graft, D. Haarer: J. Chem. Phys. **72**, 4996 (1980)
17. J. Friedrich, H. Scheer, B. Zickendraht-Wendelstadt, D. Haarer: J. Am. Chem. Soc. **103**, 1030 (1981); J. Chem. Phys. **74**, 2260 (1981)
18. A.R. Gutierrez: Chem. Phys. Lett. **74**, 293 (1980)
19. E. Gueller, G. Castro: Chem. Phys. **54**, 217 (1981)
20. R.A. Avarmaa, K.H. Mauring, A.P. Suisalu: Izv. Akad. Nauk ESSR, Fiz. Mater. **29**, 426 (1980); Chem. Phys. Lett. **77**, 88 (1981)
21. K. Mauring, R. Avarmaa: Chem. Phys. Lett. **81**, 446 (1981)
22. K.K. Rebane, R.A. Avarmaa: J. Photochem. **17**, 311 (1981)
23. V.G. Maslov: Dokl. Akad. Nauk SSSR **246**, 1511 (1979)
V.G. Maslov, A.S. Chunaev, V.V. Tugarinov: Biophysika **25**, 925 (1980)
24. D.M. Burland, D. Haarer: IBM J. Res. Dev. **23**, 534 (1979)
25. A.A. Gorokhovskii, J.V. Kikas, V.V. Palm, L.A. Rebane: Fiz. Tverd. Tela **23**, 1040 (1981)
26. B.M. Kharlamov, R.I. Personov, L.A. Bykovskaya: Opt. Commun. **12**, 191 (1974)
27. B.M. Kharmalov, R.I. Personov, L.A. Bykovskaya: Opt. Spectrosc. **39**, 137 (1975)
28. J.M. Hayes, G.J. Small: Chem. Phys. **27**, 151 (1978); Chem. Phys. Lett. **54**, 435 (1978); J. Lumin **18/19**, 219 (1979)
29. V. Bogner, R. Schwarz: Phys. Rev. B**24**, 2846 (1981)
30. F.G. Herson, H.W.H. Lee, R.W. Olson, M.D. Fayer: Chem. Phys. Lett. **84**, 59 (1981)
31. W.R. Bennet, Jr.: Phys. Rev. **126**, 580 (1962)
32. A. Szabo: Phys. Rev. B**11**, 4512 (1975)
33. V.S. Letokhov, V.P. Chebotayev: *Nonlinear Laser Spectroscopy* Springer Ser. Opt. Sci. **4** (Springer, Berlin, Heidelberg, New York 1977)
34. R.A. Avarmaa, K.H. Mauring: Opt. Spectrosc. **41**, 670 (1976)
35. R.M. Shelby, R.M. Macfarlane: Chem. Phys. Lett. **64**, 545 (1979)
36. K.K. Rebane: *Impurity Spectra of Solids* (Plenum Press, New York 1970)
37. C.P. Slichter: *Principles of Magnetic Resonance*, 2nd ed., Springer Ser. Solid-State Sci. **1** (Springer, Berlin, Heidelberg, New York 1980)
38. A.A. Gorokhovskii, J.V. Kikas: Zh. Prikl. Spektrosk. **28**, 832 (1978)
39. S. Voelker, R.M. Macfarlane, A.Z. Genack, H.P. Trommsdorff, J.H. van der Waals: J. Chem. Phys. **67**, 1759 (1977)
40. H. de Vries, D.A. Wiersma: J. Chem. Phys. **72**, 1852 (1980)
41. J. Friedrich, J.D. Swalen, D. Haarer: J. Chem. Phys. **73**, 705 (1980)
42. L.A. Rebane: Ultrafast Relaxation and Secondary Emission, Proc. Intern. Symp. "Ultrafast Phenomena in Spectroscopy", Tallinn (1978) pp. 89–112
43. A.A. Gorokhovskii, L.A. Rebane: Izv. Akad. Nauk SSSR, Ser. Fiz. **44**, 859 (1980)
44. S. Voelker, R.M. Macfarlane, J.H. van der Waals: Chem. Phys. Lett. **53**, 8 (1978)

45. M.J. Burns, W.K. Lin, A.H. Zewail: In *Molecular Spectroscopy*, a series in Modern Problems in Solid State Physics, ed. by V. M. Agranovich and R. M. Hochstrasser (North-Holland, Amsterdam 1981)
46. R.W. Olson, H.W.H. Lee, F.G. Patterson, M.D. Fayer: J. Chem. Phys. **76**, 31 (1982)
47. A.A. Gorokhovskii, L.A. Rebane: Fiz. Tverd. Tela **19**, 3417 (1977)
48. S. Voelker, R.M. Macfarlane: Chem. Phys. Lett. **61**, 421 (1979)
49. B.M. Kharlamov, L.A. Bykovskaya, R.I. Personov: Zh. Prikl. Spektrosk. **28**, 840 (1978); Chem. Phys. Lett. **50**, 407 (1977)
50. J.M. Hayes, R.P. Stout, G.J. Small: J. Chem. Phys. **74**, 4266 (1981)
51. A.A. Gorkhovskii: Opt. Spectrosc. **40**, 477 (1976)
52. A.I.M. Dicker, M. Noort, S. Voelker, J.H. van der Waals: Chem. Phys. Lett. **73**, 1 (1980)
    A.I.M. Dicker, M. Noort, H.P.H. Thijssen, S. Völker, J.H. van der Waals: Chem. Phys. Lett. **78**, 212 (1981)
53. R. Avarmaa: Izv. Akad. Nauk ESSR, Fiz. Mater. **23**, 238 (1974)
54. J. Kikas: Chem. Phys. Lett. **57**, 511 (1978)
55. A.A. Gorokhovskii, R.K. Kaarli: Izv. Akad. Nauk SSSR, Ser. Fiz. **39**, 2326 (1975)
56. P. Avouris, A. Campion, M.A. El-Sayed: J. Chem. Phys. **67**, 3397 (1977)
57. T.B. Tamm, P.M. Saari: Chem. Phys. Lett. **30**, 219 (1975)
58. J. Kikas, M. Ratsep: phys. stat. sol. (b) **112**, 409 (1982)
59. J. Kikas, K. Rebane: To be published
60. A.B. Treshchalov, L.A. Rebane: Fiz. Tverd. Tela **20**, 469 (1978)
61. D.L. Huber: In *Laser Spectroscopy of Solids*, ed. by W. W. Yen, P. M. Selzer. Topics Appl. Phys. **49** (Springer, Berlin, Heidelberg, New York 1981)
62. J. Friedrich, D. Haarer: J. Chem. Phys. **76**, 61 (1982)
63. R. Jaaniso, J. Kikas: Izv. Akad. Nauk ESSR **30**, 247 (1976)
64. B. Di Bartolo: *Optical Interactions in Solids* (Wiley, New York 1968)
65. M.A. Krivoglaz: Fiz. Tverd. Tela **6**, 1707 (1964)
66. P.M. Selzer, D.L. Huber, D.S. Hamilton, W.M. Yen, M.J. Weber: Phys. Rev. Lett. **36**, 813 (1976)
    J. Hegarty, W.M. Yen: Phys. Rev. Lett. **43**, 1126 (1979)
67. S.K. Lyo, R. Orbach: Phys. Rev. B**22**, 4223 (1980)
68. P.W. Anderson, B.J. Halperin, C.M. Varma: Philos. Mag. **25**, 1 (1972)
69. I.S. Osad'ko: Pisma ZhETF **33**, 640 (1981)
70. V. Hizhnyakov, I. Tehver: phys. stat. sol. (b) **95**, 65 (1979)
71. R.I. Personov, E.I. Al'shits, L.A. Bykovskaya, B.M. Kharlamov: ZhETF **65**, 1815 (1973)
72. A.P. Marchetti, W.C. McColgin, J.H. Eberly: Phys. Rev. Lett. **35**, 387 (1975)
73. K.N. Solov'ev, I.E. Zalesski, U.N. Kotlo, S.F. Shkirman: JETP Lett. **17**, 332 (1973)
74. G. Castro, D. Haarer, R.M. Macfarlane, H.P. Trommsdorff: US Patent No. 4, 101, 976 (1978)
75. A.A. Gorokhovskii, V.V. Palm: To be published

Note added in proof: Recently the hole burning at the forbidden $S_0 \rightarrow T_1$ transition in pyrene molecule in the glassy-like Br-butyl was observed [75]. The holewidth of 0.07 cm^{-1} was obtained when the linewidth of resonantly excited phosphorescence was equal to 0.01 cm^{-1}. This difference is apparently caused by a rearrangement of the impurity surrounding during the measurement cycle ($\sim 10^3$ s).